Cell, Vol. 94, 217–227, July 24, 1998, Copyright ©1998 by Cell Press

Degradation Signal Masking by Heterodimerization of MATα2 and MATa1 Blocks Their Mutual Destruction by the Ubiquitin-Proteasome Pathway

Phoebe R. Johnson,* Robert Swanson,†
Larissa Rakhilina,* and Mark Hochstrasser*‡
*Department of Biochemistry and Molecular Biology
†Department of Molecular Genetics and Cell Biology
University of Chicago
Chicago, Illinois 60637

Summary

Proteolysis by the ubiquitin-proteasome pathway is often regulated, but the mechanisms underlying such regulation remain ill-defined. In *Saccharomyces cerevisiae*, cell type is controlled by the *MAT* transcription factors. The α2 repressor is a known ubiquitin pathway substrate in α haploid cells. We show that a1 is rapidly degraded in a haploids. In a/α diploids, α2 and a1 are stabilized by heterodimerization. Association depends on N-terminal coiled-coil interactions between a1 and α2. Residues in α2 important for these interactions overlap a critical determinant of an α2 degradation signal, which we delimit by extensive mutagenesis. Our data provide a detailed description of a natural ubiquitin-dependent degradation signal and point to a molecular mechanism for regulated turnover in which proteolytic signals are differentially masked in alternative multiprotein complexes.

Introduction

Rapid degradation of specific cellular proteins is central to many biological regulatory mechanisms, including aspects of signal transduction, cell cycle progression, differentiation, and the stress response (Gottesman, 1996; Hochstrasser, 1996; Varshavsky, 1997). For many short-lived eukaryotic proteins, a necessary step in their degradation is covalent attachment to ubiquitin (Ub). In these conjugates, Ub is attached to a lysine side chain(s) of the substrate. Generally, attachment of a polyUb chain is necessary for efficient degradation by the 26S proteasome. Protein ubiquitination depends on a series of enzymes (Hochstrasser, 1996). Activation of the C terminus of Ub by Ub-activating enzyme (E1) is the first step in all ubiquitination pathways. Ubiquitin is then transferred from E1 to a Ub-conjugating enzyme (Ubc or E2). The E2s constitute a sizeable family of enzymes, the members of which can transfer Ub to specific substrates. The E2s usually associate with factors called E3s or Ub-protein ligases, and the E2/E3 complex appears to be responsible for substrate recognition and ubiquitination.

A fundamental question about this pathway concerns the nature of the substrate features that allow specific recognition by E2s and/or E3s. At present, only fragmentary information on the nature of such "degradation signals" is available. The first characterized signal was defined with a set of engineered proteins called N-end rule substrates (Varshavsky, 1997). The principal components of the N-end rule signal are the N-terminal residue and a conformationally accessible lysine residue that can be ligated to Ub. Short sequence motifs such as the cyclin destruction box (Glotzer et al., 1991) and stretches rich in Pro, Glu/Asp, Ser, and Thr residues called PEST sequences (Rechsteiner and Rogers, 1996) are necessary for degradation of certain Ub-dependent substrates, but they are not sufficient. The defining character of PEST elements also remains unclear. For instance, only a subset of site-directed mutations in the PEST motif of the yeast Gcn4 protein inhibited proteolysis (Kornitzer et al., 1994). While a variety of natural substrates have been analyzed using deletions or mutation of potential ubiquitination sites, no systematic random point mutagenesis has yet been done on any of them.

In several instances, Ub-dependent degradation rates of particular proteins have been shown to be regulated. Examples include the following: cyclins and the cyclin-dependent kinase inhibitors, which are destroyed at specific points in the cell cycle (King et al., 1996); IκB, an inhibitor of the NFκB transcription factor, which is degraded in response to certain extracellular signals (Yaron et al., 1997); and Gcn4, a transcription factor for amino acid biosynthetic genes that is metabolically stabilized by amino acid starvation (Kornitzer et al., 1994). Although some of the molecular events that are required for these changes in protein turnover are known (e.g., substrate phosphorylation), the exact mechanisms of switching degradation on or off are just beginning to be determined.

Our studies have focused on the α2 repressor of *Saccharomyces cerevisiae* (Chen et al., 1993; Hochstrasser, 1996). This eukaryote has three cell types: two haploid forms, **a** and α, and an **a**/α diploid, produced by mating of haploid cells of opposite cell type (Herskowitz et al., 1992). Cell identity is governed by the mating type, or *MAT*, locus. In homothallic strains, mating type can switch when **a** or α sequences from one of two unexpressed loci is copied into the *MAT* locus. The change in cellular phenotype is apparent within a single cell cycle, suggesting that the transcriptional regulators encoded by the *MAT* loci may be short-lived. In fact, we found that the α2 homeodomain protein, which is encoded by the *MAT*α locus, has an in vivo half-life of ~4 min in α cells. The Ub system is responsible for α2 degradation by mechanisms involving at least two degradation signals and four E2/Ubc enzymes. Ubc4 and Ubc5 define one proteolytic pathway, while Ubc6 and Ubc7 define the other, with the Ubc6/Ubc7-containing complex targeting the *Deg1* signal, which resides within the first 67 residues of α2 (Chen et al., 1993).

Here, we describe a high resolution mutational analysis of the *Deg1* signal, which has revealed a discontinuous signal that depends on neither the PEST motif nor the cyclin destruction box found in α2 but has as its primary determinant a 19-residue segment that forms part of a predicted amphipathic helix. This helix was previously shown to be important for formation of the **a**1-α2 heterodimer in **a**/α diploid cells. We show that

‡To whom correspondence should be addressed.

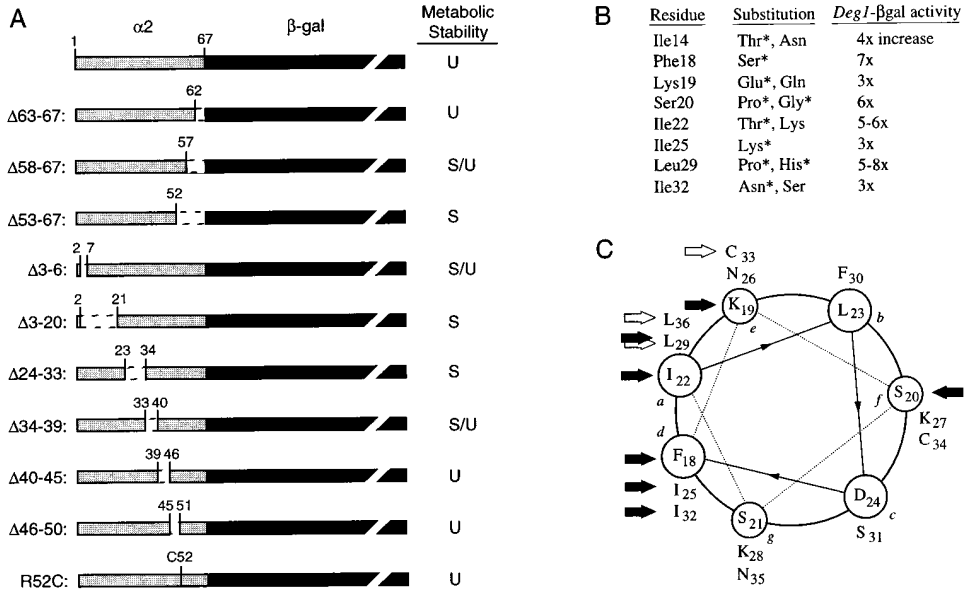

Figure 1. Mutagenesis of the *Deg1* Degradation Signal

(A) Deletion analysis of *Deg1*. Pulse-chase analysis of *Deg1*-βgal was used to evaluate degradation kinetics. S, metabolically stable ($t_{1/2} > 4\times$ wild-type); U, degradation rate similar to wild-type *Deg1*-βgal; S/U, partial stabilization ($t_{1/2}$ 2–4× wild-type). Another construct, Δ14–23, was analyzed but found to generate an abnormal cleavage product.

(B) Summary of point mutations in *Deg1* that cause defects in *Deg1*-βgal degradation. The average fold increase in βgal activity over wild-type is indicated. Residues marked with an asterisk denote mutants that were tested by pulse-chase.

(C) Helical-wheel representation of region of α2 N terminus (residues 18–36) predicted to form part of a coiled-coil structure. The hydrophobic surface may extend to residue 14, but the additional sequence does not conform to the 3,4 heptad repeat. Black arrows mark residues whose mutation inhibited *Deg1*-mediated proteolysis. Open arrows indicate residues where substitutions weaken binding to **a**1 (Ho et al., 1994).

degradation of α2 is severely inhibited in **a**/α cells. Similarly, **a**1 is short-lived in **a** cells and is strongly stabilized in **a**/α diploids. This regulation by cell type is a direct consequence of the physical association between **a**1 and α2. The results indicate that degradation determinants in **a**1 and α2 that overlap (or are closely juxtaposed to) the interaction surfaces of these two molecules are masked in the heterodimer. We anticipate that such a steric mechanism of proteolytic regulation will contribute to the degradation of many other regulatory proteins as well as misfolded or otherwise abnormal proteins.

Results

Deletion Analysis of the *Deg1* Degradation Signal of α2

Previously, we found that the first 67 residues of α2 could target normally long-lived proteins such as *Escherichia coli* β-galactosidase (βgal) for rapid degradation (Hochstrasser and Varshavsky, 1990; Chen et al., 1993). To localize the signal more precisely, small terminal α2 deletions were engineered in the context of the $\alpha2_{1-67}$-βgal protein, and degradation rates were measured by pulse-chase analysis. The results indicated that the first 62 residues of α2 were sufficient for maximal rates of *Deg1*-mediated proteolysis (half-life ~10–20 min), whereas further deletions from either end of this segment retarded degradation at least partially (Figure 1A). Two internal deletions, Δ3–20 and Δ24–33, strongly inhibited degradation, suggesting that residues within these regions are important for *Deg1* function. Δ34–39 also was impaired in degradation but to a lesser degree. In contrast, several internal stretches could be deleted without compromising degradation (Δ40–45 and Δ46–50).

The residues covered by these last two deletions involved a PEST sequence: residues 38–52 of α2 yield a PESTFIND score of 7.4 (Rechsteiner and Rogers, 1996). To test whether degradation of the PEST deletions was due to creation of a substrate for a proteolytic pathway that does not normally act on *Deg1*, we measured turnover of the Δ40–45 mutant (which lacks all the Pro, Ser, and Thr residues of the PEST element) in a *ubc6*Δ strain. Degradation of both Δ40–45 and wild-type $\alpha2_{1-67}$-βgal was strongly inhibited (data not shown). Hence, the α2 PEST sequence is not necessary for *Deg1*-mediated proteolytic targeting. The data also indicate that the *Deg1* signal is discontinuous, with residues important for degradation both upstream and downstream of the dispensable PEST region.

Another sequence implicated in substrate targeting to the Ub pathway is the cyclin destruction box (DB), a 9-residue sequence found in all the A- and B-type cyclins as well as some noncyclin proteins (King et al., 1996). Residues 52–60 of α2 show similarity to the DB, as pointed out earlier (Glotzer et al., 1991), including the two most conserved DB residues, Arg1 and Leu4. Indeed, degradation of $\alpha2_{1-67}$-βgal derivatives that lacked parts of the DB-like sequence was at least partially impaired (Figure 1A). To test DB dependence more rigorously, we mutated the critical Arg (R52 in α2) to Cys, a mutation that inactivates cyclin B degradation. The R52C mutant was degraded with the same kinetics as

wild-type $\alpha 2_{1-67}$-βgal (Figure 1A), and degradation was still severely impaired in a *ubc6*Δ mutant (data not shown), indicating that *Deg1*-mediated proteolytic targeting does not require the DB.

In summary, proteolytic targeting by the *Deg1* signal requires several discontinuous regions in the N-terminal 62 residues of α2. These determinants do not include two sequences previously implicated in Ub-dependent proteolysis, the PEST motif and the cyclin DB, even though such sequences are present in α2.

A Key Determinant of the *Deg1* Signal Localizes to a Predicted Amphipathic Helix

Deletion analysis provided a low-resolution description of the *Deg1* proteolytic signal. We therefore devised a screen to identify individual residues within *Deg1* that are critical for its function. The DNA encoding the $\alpha 2_{1-67}$ portion of $\alpha 2_{1-67}$-βgal was randomly mutagenized, and plasmids encoding mutagenized *Deg1*-βgal were tested in wild-type yeast cells (see Experimental Procedures). In a first set of experiments, mutations resulting in enhanced βgal levels clustered in five codons: L29P (isolated 8 times), F18S (6), S20P (4), I22T (3) and I22K (2), and I14T (3) (Figure 1). Subsequent mutagenesis trials yielded essentially the same substitutions with the addition of I14N and K19E (2). Significantly, the most frequently isolated mutations were again L29P (6 times), S20P (3), and F18S (3), suggesting that the repeated isolation of these alleles was a result of their strong effects on degradation. The stabilizing effect of the K19E substitution was not due to this lysine being a necessary Ub ligation site in *Deg1*-βgal. Substitution of this Lys (or of any of the other seven lysines in *Deg1* or of all eight lysines together) with a nonubiquitinatable Arg did not prevent Ubc6/Ubc7-dependent degradation (data not shown).

These results suggested that the *Deg1* residues most sensitive to mutation clustered in amino acids 14–29 of α2. To explore this region more systematically, we employed cassette mutagenesis (Reidhaar-Olson et al., 1991) to generate changes in residues 10–37 (see Experimental Procedures). Only seven mutants with elevated βgal activity that were sequenced had single mutations: K19Q and K19E, I25K, L29P and L29H, and I32S and I32N. All the residues implicated in *Deg1* function by random mutagenesis were again isolated as mutants here, with the exception of F18, but because most of these occurred in combination with other nonsilent changes, we did not analyze them further.

All of the mutations that strongly augmented βgal levels in the experiments above were shown by pulse-chase analysis to result in stabilization of *Deg1*-βgal (Figure 1B). Considered together, the data indicate that residues 14–32 make up the key determinant of the *Deg1* degradation signal. This region overlaps a prominent 3,4-heptad repeat that is predicted to form part of a coiled-coil structure (Ho et al., 1994). When the *Deg1*-inactivating mutations were mapped onto a helical wheel projection of this segment of α2, almost all the residues affected were on the hydrophobic face of the predicted amphipathic helix (Figure 1C). The alterations observed in residues at the hydrophobic *a* and *d* positions of the heptad repeat would be expected to weaken

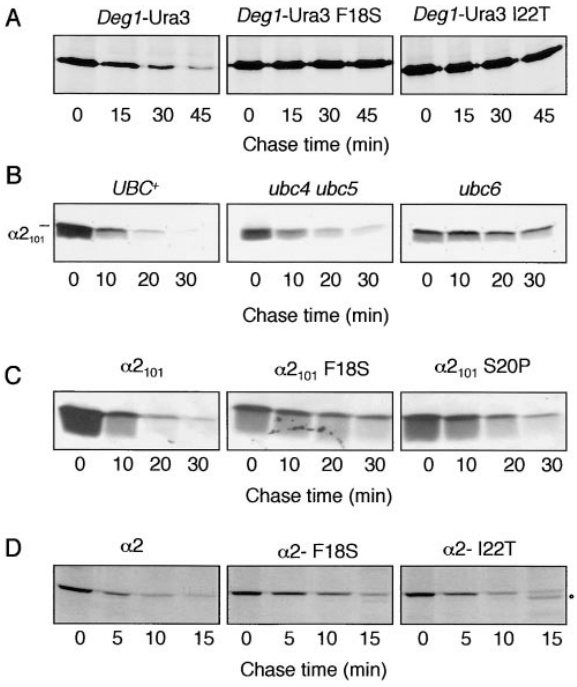

Figure 2. *Deg1*-Inactivating Substitutions Inhibit Degradation in Multiple Contexts

(A) Pulse-chase analysis in MHY501 cells of *Deg1*-Ura3 derivatives bearing point mutations in *Deg1*. Proteins were precipitated with antibodies against α2.

(B) Pulse-chase analysis of $\alpha 2_{101}$ in ubiquitin pathway mutants. MHY501, MHY508, or MHY495 cells carried a high-copy plasmid expressing $\alpha 2_{101}$. The protein is 5- to 6-fold more stable in MHY495 cells than in either MHY501 or MHY508.

(C) Pulse-chase analysis in MHY501 cells of $\alpha 2_{101}$ derivatives.

(D) Pulse-chase analysis in MHY1147 cells of full-length α2 derivatives. Asterisk marks an aberrant α2-I22T fragment (which can also be detected for α2-F18S).

coiled-coil interactions. The K19 mutations affected a residue at the *e* position. Residues at the *e* and *g* positions of heptad repeats often help stabilize the interhelical interface (Lupas, 1996). The S20P mutation mapped to the outside surface of the predicted helix, but proline can act as a helix breaker.

In a preliminary set of studies, we chose three of the most frequently mutated residues, F18, S20, and I22, and incorporated random nucleotides in the corresponding codons such that 14 or 15 different amino acids could be encoded at each position. Only S20P and S20G mutations were isolated among the blue colonies from the S20 mutagenesis. The S20G mutation also inhibited *Deg1*-βgal degradation based on pulse-chase analysis (Figure 1B). Gly, like Pro, is often a helix breaker. The analysis of this data set remains incomplete, but it is clear that positions 18 and 22 generally only tolerate hydrophobic residues, consistent with a role in a coiled-coil motif (data not shown).

We determined whether any of the mutations that inactivated *Deg1* in the *Deg1*-βgal fusion had an effect on turnover of other *Deg1*-containing proteins. Representative mutations were introduced into *Deg1*-Ura3, $\alpha 2_{101}$ (the 101-residue globular N-terminal domain of α2

[Sauer et al., 1988]), and full-length α2. Figure 2A shows that, as with *Deg1*-βgal, the F18S and I22T mutations greatly impeded *Deg1*-Ura3 degradation, indicating that their inhibitory effects were not dependent on the large, tetrameric βgal reporter. We engineered the $\alpha2_{101}$ protein to create what should be an independent folding domain of α2 that is free of heterologous protein sequences. Like α2, the truncated protein is short-lived in yeast, with a half-life of ~5–6 min; its degradation is strongly dependent on the *Deg1*-mediated Ubc6/Ubc7 pathway but not the Ubc4/Ubc5 pathway (Figure 2B). Correspondingly, the F18S and S20P mutations in the *Deg1* signal inhibited $\alpha2_{101}$ degradation ~3- to 4-fold (Figure 2C).

Degradation of full-length α2 depends less on a single Ubc pathway than do either *Deg1* fusions or $\alpha2_{101}$. For example, deletion of *UBC6* and/or *UBC7* slows α2 degradation by only ~2-fold (Chen et al., 1993). Consistent with this, the *Deg1*-inactivating F18S mutation had a modest (1.2- to 1.6-fold) effect on α2 turnover (Figure 2D). In contrast, degradation of α2-I22T was similar to wild-type α2. For α2-I22T, an aberrant cleavage product accumulated (Figure 2D), and unlike wild-type α2, which is stabilized 10- to 15-fold in *ubc4 ubc6* cells, α2-I22T was still degraded rapidly in the mutant (data not shown). The α2-F18S protein was longer-lived in *ubc4 ubc6* ($t_{1/2} > 15$ min), although the effect appeared to be less pronounced than with wild-type α2. We conclude that the F18S mutation impairs *Deg1* function in full-length α2, but *Deg1* function in α2-I22T cannot be evaluated because the mutant is degraded by a pathway(s) that does not act on wild-type α2.

Collectively, the mutagenesis data reveal a striking clustering of inactivating mutations within *Deg1*, and these alterations localize primarily to the hydrophobic face of a predicted amphipathic helix.

Degradation of α2 Is Strongly Inhibited in a/α Diploid Cells

Independent evidence for an N-terminal amphipathic helix in α2 was obtained by Ho et al. (1994), who showed that mutations predicted to alter this helix disrupted binding of α2 and **a**1 in vitro and in vivo (see Figure 1C). Therefore, overlapping segments of α2 are involved in both Ub-dependent proteolysis and **a**1 interaction. Previous studies of α2 turnover were carried out almost entirely in α haploid cells. Remarkably, when assayed in **a**/α diploid cells, α2 degradation was dramatically reduced relative to haploids (Figure 3A). A detailed kinetic analysis of α2 degradation in **a**/α diploids revealed an initial period during which degradation approached the rate observed in haploid α cells, followed by an extended period with very little degradation (Figure 3B). In different experiments, degradation plateaued after 10–15 min with ~25%–35% of the radiolabeled α2 protein remaining.

We considered three general models that could account for the drastic change in α2 degradation kinetics observed between α haploid and **a**/α diploid cells. First, these two cell types differ in ploidy, so a difference in dosage of one or more genetic loci may affect a component(s) of the α2 proteolytic system. Second, the **a**1-α2 transcriptional repressor changes the pattern of gene expression in **a**/α cells, and this could reduce or eliminate a component of the Ub-proteasome pathway that is important for α2 turnover. Finally, the physical association of the **a**1 polypeptide with α2 could interfere with the targeting of α2 for ubiquitination or degradation.

To test the effect of ploidy on α2 turnover, cells expressing one or both of the *MAT* loci were analyzed. Degradation of α2 was strongly inhibited in haploid α cells that had been transformed with a plasmid carrying *MAT***a** (Figure 3C). In the complementary experiment, α2 degradation was measured in *mat***a**1/*MAT*α diploids. In these cells, which lack **a**1 protein, α2 was degraded with the same kinetics previously observed in α haploid cells (data not shown). These results demonstrate that coexpression of **a**1 and α2, rather than chromosome ploidy, regulates degradation of the α2 repressor.

Formation of the **a**1-α2 repressor turns off transcription of the haploid-specific genes regardless of cell ploidy (Hersko itz et al., 1992). Although the **a**1-α2 heterodimer is sufficient for sequence-specific DNA binding, transcriptional repression also requires the general repressor complex Tup1-Ssn6 (Herskowitz et al., 1992). We found that proteolysis of α2 continued to be markedly inhibited in *tup1*Δ *ssn6*Δ cells (MHY478) expressing both α2 and **a**1; in addition, α2 mutants bearing an I4T or L10S substitution, which are defective for Tup1 association (Komachi et al., 1994), were still stabilized by **a**1 (data not shown). These data (and experiments with $\alpha2_{101}$; see below) demonstrate that transcriptional regulation by the **a**1-α2 complex is not required for **a**1-dependent stabilization of α2.

In summary, neither the difference in ploidy nor in the distinct transcriptional programs of α versus **a**/α cells can account for the striking difference in α2 degradation kinetics between these two cell types. The third model proposes that the direct binding of **a**1 to α2 alters the susceptibility of α2 to Ub-dependent proteolysis in vivo. We describe strong evidence in support of this idea in a later section.

The a1 Protein Is Short-Lived in a Cells and Is Metabolically Stabilized in a/α Cells

By the same logic that α2 was initially predicted to be degraded rapidly in α cells (see Introduction), the **a**1 protein would be expected to be short-lived in **a** cells. Indeed, we found that **a**1 was destroyed exceptionally rapidly in **a** haploid cells (Figure 3D). We do not yet know many details about the mechanism of **a**1 turnover, but in *ubc4 ubc6* and *doa4* mutants (Hochstrasser, 1996), degradation of **a**1 was inhibited by at least 3-fold and 6-fold, respectively, relative to wild-type (data not shown). Hence, the Ub-proteasome pathway is also crucial for **a**1 breakdown. Examination of **a**1 degradation in **a**/α cells revealed that its turnover was regulated by cell type in the same manner as α2. The half-life of **a**1 increased from well under a minute in **a** haploids to over 15 min in **a**/α cells (Figure 3D). The **a**1 protein was also metabolically stabilized in **a** haploid cells carrying *MAT*α on a plasmid, but not in diploid cells deleted for *MAT*α*2* (data not shown).

Physical Association of a1 and α2 Prevents Their Mutual Destruction

The biphasic kinetics of α2 degradation in **a**/α cells (Figure 3B) suggested the presence of two metabolically

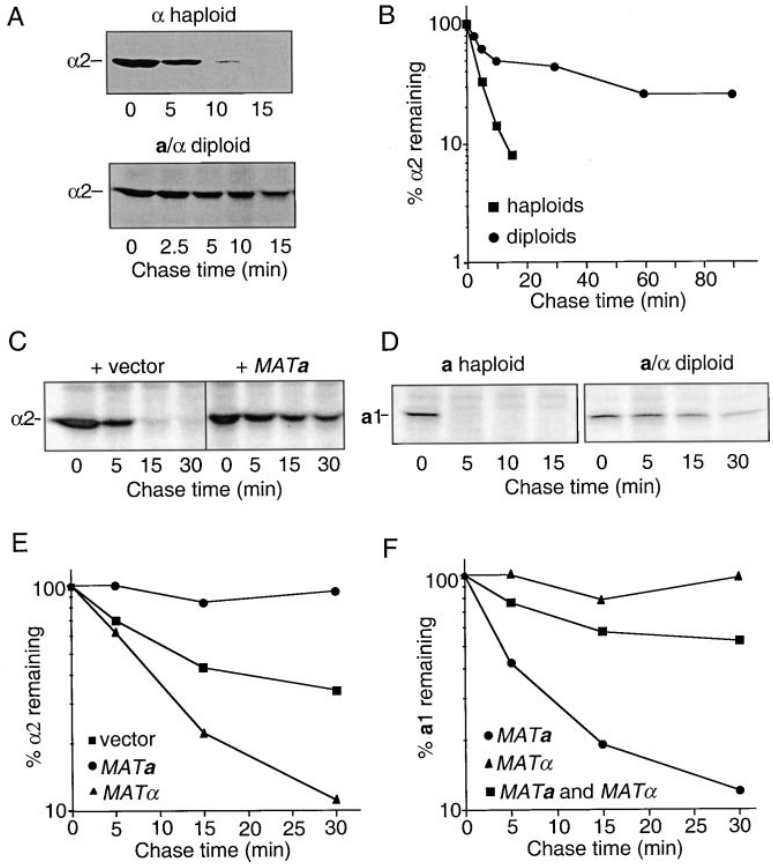

Figure 3. Regulation of α2 and **a**1 Degradation by Cell Type

(A) Pulse-chase analysis of α2 degradation in α haploid (MHY489) and **a**/α diploid (MHY949) cells.

(B) Detailed kinetic analysis of α2 turnover in **a**/α diploids. Pulse-chase analysis in MHY949 was done with three simultaneous pulse-chases having overlapping time points.

(C) MATα2 is metabolically stabilized in α haploid cells carrying a *MAT***a** plasmid. Pulse-chase analysis of α2 in MHY479 cells carrying YCplac111 or YCplac111-MAT**a**.

(D) Rapid degradation of **a**1 in **a** cells but not **a**/α diploids. Pulse-chase analysis of endogenous **a**1 in wild-type **a** haploid (MHY488) and **a**/α diploid (MHY949) cells. Proteins were precipitated with an antiserum against **a**1.

(E) Altering relative levels of **a**1 and α2 changes the rate of α2 degradation. Degradation of α2 assayed in MHY949 cells carrying the indicated high-copy plasmid-borne *MAT* alleles.

(F) Altering relative levels of **a**1 and α2 changes the rate of **a**1 degradation. Degradation of **a**1 in MHY949 cells carrying the indicated high-copy plasmid-borne *MAT* alleles.

distinguishable populations of α2 molecules in these cells. In this view, rapid disappearance of α2 at early chase time points reflects efficient degradation of α2 homodimers (and/or monomers), as occurs in α haploids. The fraction of α2 bound to **a**1 would represent a second pool of α2 in **a**/α cells that is only slowly degraded during the chase. This interpretation predicts that changing the relative levels of **a**1 and α2 should lead to changes in the degradation kinetics of α2 (and **a**1). To test this, **a**1 was overproduced from a *MAT***a**-containing plasmid in **a**/α diploids in an attempt to force more of α2 into the **a**1-α2 heterodimer pool. As predicted, degradation of α2 was further retarded in these cells compared to the same cells transformed with control plasmid (Figure 3E). Conversely, when *MAT*α was overexpressed in **a**/α diploids to increase the fraction of α2 present as monomer or homodimer, a larger fraction of labeled α2 was degraded than in the control (Figure 3E). These data strongly support the idea that two distinct pools of α2 protein exist in **a**/α cells and also imply that dissociation of α2 from the **a**1-α2 heterodimer must be relatively slow in vivo. In an analogous set of experiments, we found that **a**1 was metabolically stabilized when α2 was present in large amounts relative to **a**1 (Figure 3F). Conversely, a larger fraction of **a**1 was short-lived when it was expressed in excess relative to α2. Hence, altering the relative levels of **a**1 and α2 proteins changes the degradation kinetics of both proteins in a way consistent with mutual stabilization of **a**1 and α2 through heterodimer formation.

To examine more directly whether the physical interaction of **a**1 with α2 inhibits α2 degradation, α2 point mutants defective for **a**1 binding were analyzed. These mutants were shown previously to be severely impaired in **a**1 interaction in vitro and **a**1-α2 repression in vivo; because the mutants are nearly wild-type for α2 homodimer function, they are not likely to be grossly misfolded (Ho et al., 1994; Vershon et al, 1995; data not shown). Two of the three mutations analyzed, α2-L29R and α2-C33Y, map to the N-terminal-most amphipathic helix of α2. The third, α2-L196S, maps to a region C-terminal to the homeodomain (Li et al., 1995). None of the mutants, when expressed from low-copy plasmids, could repress transcription of **a**1-α2 target genes (data not shown).

Plasmids encoding either wild-type or mutant α2 proteins were introduced into *MAT***a**/*mat*α*2*$^{-}$ diploid cells, and the degradation rates of plasmid-expressed α2 and endogenous **a**1 were determined by pulse-chase analysis. Unlike wild-type α2, the two α2 proteins with the N-terminal substitutions were rapidly degraded, whereas the C-terminal mutant α2-L196S was still partially stabilized (Figure 4A). Strikingly, the defects in α2 stabilization in these cells were accompanied by quantitatively similar effects on **a**1 turnover: **a**1 was rapidly degraded in cells expressing α2-L29R or α2-C33Y and degraded at a rate intermediate between the normal **a** cell and **a**/α cell rates in cells expressing α2-L196S (Figure 4B). Thus, disrupting interactions between **a**1 and the N-terminal domain of α2 strongly interferes with cell type–regulated degradation of **a**1 and α2. In contrast, disrupting the **a**1-α2 C-terminal interaction causes a more modest defect in regulation.

Because mutations in α2 can have unforeseen effects on in vivo proteolysis, we tested the degradation kinetics

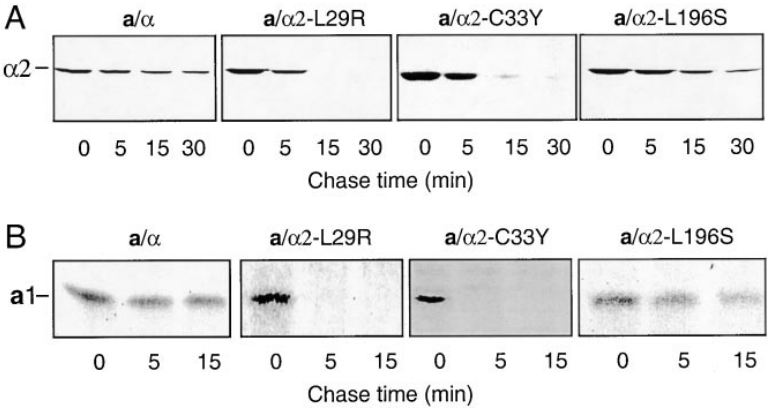

Figure 4. Degradation of **a**1 Interaction–Defective α2 Proteins in the Presence of **a**1

(A) Degradation of mutant α2 proteins in **a**/α diploids. Pulse-chase analysis was done in *MAT***a**/*matα2*$^-$ cells (MHY940) with low-copy plasmids expressing wild-type α2, α2-L29R, α2-C33Y, or α2-L196S.

(B) Degradation of **a**1 in same cells as in (A).

of the three **a**1-binding mutants in wild-type and *ubc4 ubc6* haploid cells (Table 1). Degradation of α2-C33Y and α2-L196S was inhibited similarly to wild-type α2 in *ubc4 ubc6* cells, but α2-L29R (and α2-L29H) turnover was only impeded ~2-fold in the double mutant, indicating that α2-L29R is targeted to a proteolytic pathway(s) that does not act on wild-type α2. (The α2-C33Y protein was degraded slightly slower than α2 in wild-type cells [$t_{1/2}$ ~8 min], but this is not due to inactivation of *Deg1* because *Deg1*-C33Y-βgal is degraded at the same rate as wild-type protein [data not shown].) Therefore, the α2-C33Y and α2-L196S data indicate that binding of **a**1 to α2 retards normal α2 degradation. For α2-L29R, proteolytic targeting of the mutant α2 could involve a mutant protein-specific pathway that may not be sensitive to **a**1 binding. These results emphasize the importance of having information on the proteolytic pathways that act on wild-type α2 for interpreting data on mutated substrates.

The $\alpha2_{101}$ protein was used to determine whether the N-terminal globular domain of α2 alone could be stabilized by **a**1. Degradation of $\alpha2_{101}$ was markedly reduced in cells expressing **a**1 (Figure 5A). In the absence of **a**1, only ~7% of the radiolabeled $\alpha2_{101}$ remained after just 15 min, whereas ~30% was still present at 30 min when **a**1 was expressed from a low-copy plasmid (Figure 5A), and over 70% remained at 30 min when **a**1 was made from a high-copy plasmid (data not shown). In the same cells, degradation of **a**1 was severely retarded in the presence of $\alpha2_{101}$ (Figure 5B). Because the $\alpha2_{101}$ domain is not known to interact with the C-terminal domain of **a**1, these results suggest that the primary **a**1 degradation signals are in the N-terminal portion that binds $\alpha2_{101}$. Inasmuch as $\alpha2_{101}$ lacks the α2 DNA binding domain and cannot repress either **a**- or haploid-specific gene transcription (data not shown), these data provide further evidence that transcriptional repression by **a**1-α2 is not required for mutual stabilization. Taken together, our data demonstrate that degradation of **a**1 and α2 is controlled by the direct physical interaction between these two proteins.

Table 1. Degradation of α2 Point Mutants

α2 Allele	Half-Life[a]	
	Wild-Type	*ubc4 ubc6*
Wild-type	4 min	44 min
L29R	4 min	9 min
C33Y	8 min	43 min
L196S	4 min	51 min

[a] Wild-type, MHY1147; *ubc4 ubc6*, MHY1131.

The a1 Protein Interferes with $\alpha2_{101}$ Ubiquitination

Binding of **a**1 to α2 may inhibit degradation at any of several steps in the proteolytic pathway. Association with **a**1 could prevent α2 ubiquitination, it could block dissociation of ubiquitinated α2 from **a**1-α2 complexes, and/or it might impair degradation of ubiquitinated α2 by the proteasome. To determine whether **a**1 prevents α2 ubiquitination, we assayed modification of $\alpha2_{101}$; $\alpha2_{101}$ is stabilized by **a**1 in the same manner as α2, but it is easier to detect ubiquitinated forms of $\alpha2_{101}$ than of α2. Lysates of radiolabeled cells expressing $\alpha2_{101}$ and either Ub or myc epitope–tagged Ub were precipitated with anti-α2 antibodies, and proteins were separated on SDS gels (Ellison and Hochstrasser, 1991). Both monoubiquitinated and diubiquitinated forms of $\alpha2_{101}$ were readily detected as species that migrated more slowly than $\alpha2_{101}$; these species contained Ub since their sizes increased when Ub was replaced by mycUb (Figure 5C, lanes 1–2). When a high-copy plasmid expressing **a**1 was introduced into the same cells, $\alpha2_{101}$ ubiquitination was strongly inhibited (lanes 3–4). Hence, the **a**1-dependent block to $\alpha2_{101}$ degradation is associated with a large decrease in $\alpha2_{101}$ ubiquitination.

Discussion

In this study, we have shown that the key determinant within a natural Ub-dependent degradation signal is the hydrophobic surface of an amphipathic helix, which is likely to be recognized by the Ubc6/Ubc7 ubiquitination pathway. This amphipathic helix also participates in a coiled-coil interaction with a second short-lived protein, and both proteins are metabolically stabilized when they form heterodimers. The data suggest a steric model for regulated degradation in which degradation determinants near or overlapping a protein–protein interface can be masked in the heteromultimer. Such a mechanism provides a simple molecular switch that determines the activity of a degradation signal. As discussed

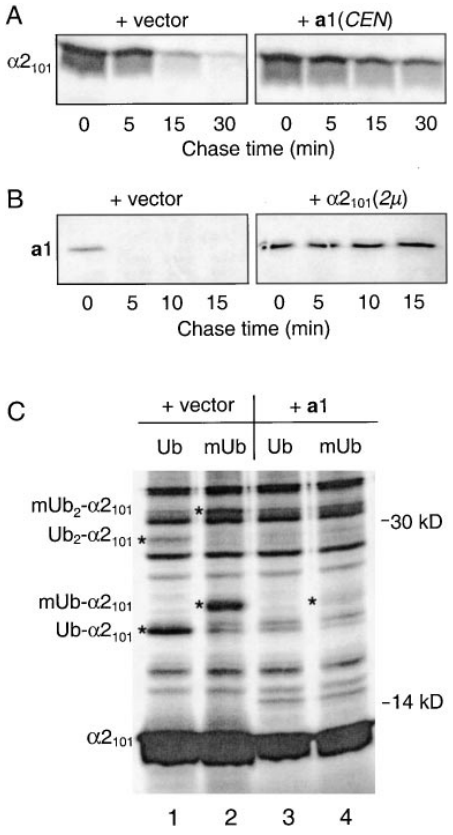

Figure 5. Degradation of $\alpha2_{101}$ Is Regulated by **a**1, and $\alpha2_{101}$ Blocks Degradation of **a**1

(A) Inhibition of $\alpha2_{101}$ degradation by **a**1. Pulse-chase analysis of $\alpha2_{101}$ in *mat*$\alpha2^-$ haploid cells (MHY1147) transformed with empty vector or YCplac22-**a**1; the latter carries an ***a1*** PCR product.

(B) Inhibition of **a**1 degradation by $\alpha2_{101}$. Pulse-chase analysis of endogenous **a**1 in **a** haploid cells (MHY488) carrying an empty high-copy vector or YEplac195-$\alpha2_{101}$.

(C) Detection of ubiquitinated species of $\alpha2_{101}$ in radiolabeled MHY486 cells in the presence or absence of **a**1. Cells contained YEplac195-$\alpha2_{101}$ as well as either YEp13 or YEp13-**a**1 and a plasmid expressing either Ub or myc epitope–tagged Ub (mUb). Monoubiquitinated and diubiquitinated species are marked by asterisks; they are absent in cells not expressing $\alpha2_{101}$ (data not shown).

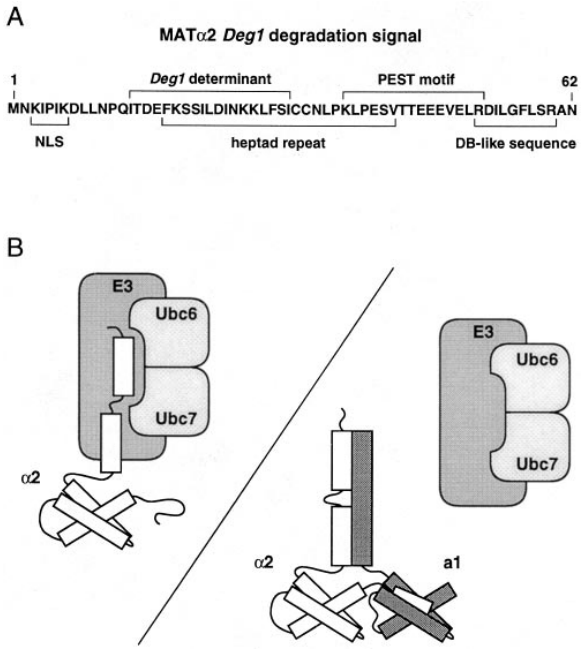

Figure 6. Model for Cell Type–Specific Regulation of MATα2 Degradation

(A) Summary of sequence elements tested for role in *Deg1*-mediated degradation by the ubiquitin-proteasome pathway. NLS, nuclear localization sequence. DB, destruction box.

(B) Model for regulated turnover. In α cells (left), the *Deg1* signal of α2 is accessible to the E2s and (predicted) E3 that recognize *Deg1*. In **a**/α diploid cells (right), **a**1 binding to α2 blocks the α2 degradation signals, preventing α2 ubiquitination. At the same time, presumptive **a**1 degradation signals are blocked by α2 binding.

below, these findings are relevant to a wide range of regulatory mechanisms involving selective protein degradation.

Degradation Signals for the Ub-Proteasome Pathway

Many natural substrates for the Ub-proteasome pathway have been identified, but the substrate features that are recognized remain ill-defined in virtually all cases. Although the basis of substrate recognition will likely differ between substrates, common features among at least some substrates can be anticipated. We have localized a key determinant of the α2 *Deg1* degradation signal to a predicted amphipathic helix (Figure 6A). Interestingly, an amphipathic helix important for proteolysis was also suggested by work from Sadis et al. (1995), who fused random peptides to the N terminus of βgal in a screen for artificial degradation signals in yeast. The PB29 peptide, which created a moderately short-lived βgal fusion protein, could be modeled as an amphipathic helix, and mutagenesis experiments supported such a structure. Degradation of this fusion protein was dependent on both Ubc6 and Ubc7, as is true for *Deg1*-mediated degradation, but unlike *Deg1*, PB29-targeted degradation also required Ubc4/Ubc5. Although no 3-D structural data are available for either of these signals, our mutagenesis results and those of Ho et al. (1994) strongly support the inference of such a helix in α2. Moreover, circular dichroism studies of the N-terminal domain of α2 indicate a largely α-helical structure (E. Reisinger and C. Wolberger, personal communication).

For the *Deg1* degradation signal, residues forming the hydrophobic face of an N-terminal amphipathic helix are the most sensitive to mutation. The most straightforward interpretation of the mutagenesis data is that this hydrophobic surface is a primary recognition element for the Ubc6/Ubc7-containing ubiquitination complex (Figure 6B). Additional residues also contribute to degradation, although they may not participate directly in E2/E3 recognition. Near the N terminus of *Deg1* is a nuclear localization sequence (NLS) (Hall and Johnson, 1987), and the Δ3–6 deletion, which prevents accumulation of *Deg1*-βgal in the nucleus (R. S. and M. H., unpublished data), confers a partial defect in degradation (Figure 1A). The NLS may help localize α2 to the nuclear periphery, where the Ubc6 and Ubc7 enzymes are concentrated

(see Sommer and Wolf, 1997). In the context of *Deg1*-βgal, residues 53–62 are also necessary for rapid degradation. How this latter segment contributes to the *Deg1* signal is not known. No inactivating point mutations were found in this region by random mutagenesis. The segment may ensure accessibility of the amphipathic helix determinant or may promote Ub transfer to α2 at some step other than E2/E3 binding.

Ubc6 and Ubc7 have recently been implicated in the degradation of both endoplasmic reticulum (ER) membrane proteins and abnormal ER luminal proteins (Sommer and Wolf, 1997). These ER proteins appear to be retrotranslocated to the cytosol following (or during) ubiquitination by the ER-localized E2 enzymes. While being ejected from the ER, such (unfolded) substrates are likely to expose, at least transiently, hydrophobic stretches that are normally in contact with the lipid bilayer or are part of protein core regions. Our data on *Deg1* suggest that such hydrophobic surfaces could be the targets for the Ubc6/Ubc7 ubiquitination machinery. The (poly)Ub tag presumably targets ER proteins to the cytosolic proteasome; it may also help to prevent the retrotranslocating proteins from slipping back into the ER.

Mechanism of Regulated Degradation of a1 and α2

The presence of **a**1 greatly retards the degradation of α2 in **a**/α cells, and a symmetrical regulation of **a**1 by α2 is observed in these same cells. Our data demonstrate that it is the direct physical interaction between these two proteins, rather than the changes in transcription caused by **a**1-α2, that is responsible for this regulation. Supporting this conclusion, *Deg1*-βgal, which does not interact efficiently with **a**1 (Hall and Johnson, 1987), is degraded at the same rapid rate in **a** haploids, α haploids, and **a**/α diploids (data not shown). Furthermore, if the cross-stabilization of **a**1 and α2 were due to the **a**/α state per se, their degradation should not have been altered by manipulations of their relative levels. Conversely, the α2 repressor continues to be metabolically stabilized in **a**/α *tup1 ssn6* cells, which are severely compromised for **a**1-α2–mediated repression. Significant stabilization by **a**1 is also observed for α2-L196S and $\alpha2_{101}$, neither of which can repress transcription with **a**1. Together, these data demonstrate that the **a**/α genetic program is neither necessary nor sufficient for **a**1-mediated stabilization of α2.

Disruption of the N-terminal associations between the **a**1 and α2 proteins has a much more severe effect on proteolytic regulation than does alteration of the C-terminal interaction site. Hence, the N-terminal interactions appear to be more critical for regulating proteolysis, an inference underscored by the finding that the isolated N-terminal domain of α2, $\alpha2_{101}$, is metabolically stabilized by **a**1 and, more surprisingly, can almost completely block degradation of full-length **a**1. An additional amphipathic helix in α2, comprising residues 67–95, is also important for **a**1 binding (Ho et al., 1994). Consistent with the above findings, the α2-L81R mutant, which is mutated in this second helix and is defective for **a**1 binding (Ho et al., 1994), is also no longer protected from degradation by **a**1 (data not shown). In addition, substitutions that alter the hydrophobic face of the predicted amphipathic helix in **a**1 also interfere with the cross-stabilization of **a**1 and α2 (P. R. J. and M. H., unpublished results). Thus, all of the analyzed mutations that disrupt the **a**1-α2 coiled-coil interface are defective in the mutual stabilization of **a**1 and α2 in vivo.

Although we cannot completely exclude the possibility that **a**1 binding somehow alters the conformation of α2 in a way that inactivates *Deg1* irrespective of exposure of the signal in the heterodimer, the direct overlap of segments of α2 implicated in both **a**1 binding and *Deg1* function makes it far more likely that binding to **a**1 directly masks at least a portion of the *Deg1* signal from the Ub pathway. The **a**1-binding surface and *Deg1* signal are nevertheless distinguishable. This is most clearly shown by the normal retardation of α2-F18S degradation by **a**1 and, conversely, the inability of the C33Y mutation to inactivate *Deg1* in a *Deg1*-βgal fusion. Interestingly, the degree to which **a**1 inhibits α2 degradation indicates that **a**1 binding interferes not only with *Deg1* but also with other α2 degradation signals. Deletion of *UBC6* and/or *UBC7* increases the half-life of α2 only 2- to 3-fold (Chen et al., 1993), whereas **a**1 overexpression nearly eliminates α2 degradation. Mapping of these additional signals is in progress.

The mechanism of regulated turnover of α2 and **a**1 is reminiscent of a model for regulation of E2F1 degradation by the retinoblastoma (Rb) protein (Campanero and Flemington, 1997). The E2F1 transcription factor is a relatively short-lived protein and is stabilized ~2-fold when Rb protein is overproduced in the same transient transfectant. The Rb-interacting domain of E2F1 overlaps an apparent C-terminal degradation signal, although it has not yet been established whether the same ubiquitination pathway targets both E2F1 and the E2F1 fusion proteins used to define this signal. Another example relevant to our data is the degradation in the ER of the T cell receptor complex α subunit, which occurs only when it is not complexed with the CD3-δ subunit of the complex (Bonifacino et al., 1990). A transmembrane region of α that is important for α-CD3-δ interactions also is involved in the degradation of the uncomplexed α subunit.

Cross-stabilization of **a**1-α2 in **a**/α cells, a phenomenon not anticipated from earlier genetic studies, may serve several functions. Inhibition of degradation may allow sufficient **a**1-α2 repressor to accumulate for repression of haploid-specific genes. This appears to be especially pertinent for **a**1, which would otherwise be degraded so rapidly ($t_{1/2} < 1$ min) that very little could accumulate. The **a**1-α2 repressor is required for initiating the meiotic pathway, but whether it continues to function later is unknown. Thus, another potential function for **a**1-α2 stabilization might be to sustain sufficient **a**1-α2 activity for completion of spore formation and/or for making spores competent for germination after cotranscription of *MAT**a1*** and *MATα2* has ceased.

Regulation of Proteolysis by Protein–Protein Interactions

The coiled coil or leucine zipper is among the best characterized and most widespread protein–protein interaction motifs (Lupas, 1996). Coiled coils mediate interactions between a number of proteins that are known to

be short-lived, including c-Jun homodimers, Fos-Jun heterodimers, and Gcn4 homodimers (Kornitzer et al., 1994; Treier et al., 1994). Whether any of the degradation signals in these proteins involves the heptad repeats is not yet clear. Coiled coils may also be involved in the degradation of normally long-lived proteins. Keratin filaments are made up of two heterologous subunits that assemble into coiled-coil structures, but when one subunit is produced in excess over its partner, the excess protein is degraded (Magin et al., 1998). By analogy to the data on regulated α2 degradation, turnover of keratin monomers may depend on accessibility of a hydrophobic surface in an unpaired amphipathic helix.

In support of this analogy, Ubc6/Ubc7-dependent ubiquitination has been implicated in the degradation of another protein that is normally part of a multisubunit complex. The Ndc10 protein forms part of the yeast kinetochore, but in *ndc10-2* mutant cells, it appears that Ndc10-2 protein is not efficiently incorporated into kinetochore complexes at the restrictive temperature, apparently causing the unincorporated protein to be rapidly degraded (Kopski and Huffaker, 1997). Mutation of *UBC6* or *UBC7* suppresses this defect. We suggest that exposure of a cryptic degradation signal overlapping a kinetochore interaction site of Ndc10 is responsible for the rapid degradation of the unincorporated subunit. More generally, "aberrant" proteins, which are often rapidly destroyed by the Ub pathway, may be identified as such by the cell based on their exposure of hydrophobic surfaces normally buried in protein–protein interfaces or within protein interiors. Our data on **a**1-α2 suggest that the principles of substrate recognition for natural and aberrant substrates of the Ub-proteasome pathway may often be similar.

The involvement of a coiled-coil motif in substrate targeting to the Ub-proteasome pathway raises the issue of how this sequence participates in the degradation process. Because interaction with **a**1 blocks α2 ubiquitination, it is possible that the α2 amphipathic helix provides a binding site for the ubiquitination complex. An obvious idea is that the E3 or E2/E3 complex includes an amphipathic helix that forms a coiled coil with the substrate. At the very least, a hydrophobic binding site in the ubiquitination complex or in another factor important for substrate recognition is implied. Direct proteasomal interrogation of the substrate portion of a polyubiquitinated protein may also occur. The c-Fos bZIP protein is rapidly degraded by the Ub-proteasome pathway, and the leucine zipper has been shown to interact with the coiled-coil motif of one the 26S proteasome ATPase subunits (Wang et al., 1996). All six ATPase subunits of the proteasome have potential coiled-coil regions. A switch from polyUb-mediated binding of the substrate to a direct proteasome–substrate interaction may allow deubiquitination and commitment of the substrate to proteolysis.

Potential for Developmental Regulation of Multisubunit Proteins

In numerous developmental pathways, a particular regulatory protein can participate in different multimeric complexes. Embryonic development in *Drosophila melanogaster* serves as an instructive example. Many transcription factors that help establish morphological pattern in the early embryo are composed of distinct sets of homeodomain proteins, not unlike the mating-type factors in yeast (Mann and Chan, 1996). These proteins are often first produced fairly broadly throughout the embryo and only subsequently focus into stripes or other patterns; such patterning depends in part on rapid substrate proteolysis in the interstitial regions (e.g., of ftz) (Kellerman et al., 1990). When coupled to transcriptional controls, selective stabilization and subunit-specific degradation of different multimers could help establish precise patterns of protein expression. As a simple illustration, if three short-lived proteins, A, B, and C, are initially expressed in overlapping regions of the embryo and can form all possible heterodimers and homodimers, but only the A-C dimer shows mutual stabilization of subunits, then the only species that will accumulate to high levels will be this heterodimer. If A-C also represses transcription of A and B, then a pattern would be created in which A-C persists along with a small dynamic population of C-C homodimers but no other species. Thus, an initially complicated and unsynchronized protein expression pattern can be resolved into a very specific and stable pattern with the aid of this simple proteolytic control. That such a mechanism is possible in vivo is indicated by the analysis of **a**1 and α2 homeodomain protein degradation presented here.

Experimental Procedures

Yeast and Bacterial Methods

Yeast rich and minimal media were prepared as described, and standard genetic methods were used (Ausubel et al., 1989). *E. coli* strains used were MC1061 and JM101, and standard techniques were employed for recombinant DNA work (Ausubel et al., 1989).

Plasmid and Strain Constructions

HindIII fragments carrying either the *MAT*α or *MAT***a** loci (Tatchell et al., 1981) were subcloned into low- and high-copy shuttle plasmids. The 5′ primer used for *α2* and $\alpha 2_{101}$ PCR amplifications annealed 200 bp upstream of the *α2* start and added a KpnI site; the 3′ primer for amplifying full-length α2 annealed 200 bp downstream of the α2 stop codon and introduced a HindIII site. The 3′ primer used to amplify $\alpha 2_{101}$ introduced a stop codon immediately after codon 101 and a BamHI site. For amplification of *MAT**a1*** sequences, we used a 5′ primer that annealed 150 bp upstream of the ***a1*** start codon and added a BamHI site and a 3′ primer that annealed 150 bp downstream of the stop codon and added a HindIII site. All PCR fragments were checked by DNA sequencing.

The *matα2-L29R* allele (Ho et al., 1994) was amplified by PCR with the *MAT*α primers described above, digested with Kpn1 and HindIII, and subcloned. The *matα2-C33Y* allele was subcloned from pKK4 (Harashima et al., 1989). To place the *matα2-L29R* and *-C33Y* mutations into equivalent contexts, DNA fragments containing these alleles were recombined in MHY481 (Table 2) with Xho-linearized YCplac111-αX38, a plasmid carrying the *matαX38* insert (Tatchell et al., 1981). Plasmids that had recombined with the homologous DNA fragments were recovered in *E. coli*, and the entire *MATα2* ORF was sequenced. Mutant α2-L196S was expressed from pAV115 (Vershon et al., 1995)

The MHY892 strain was made by mating MHY487 and MHY489. MHY940 was made by mating MHY488 to MHY486 cells that had been transformed with the YCplac33-MATα plasmid followed by eviction of the *MAT*α plasmid. MHY488 was crossed to MHY489 to make MHY949. For the *matα2::LEU2* allele, a 2 kb *LEU2*-containing SalI fragment was inserted into YCplac111-αX38 (Chen et al., 1993)

Table 2. Yeast Strains

Strain	Genotype	Source
MHY478	*MAT*α *mf**a**2:lacZ trp1 leu2 ura3 his4 ssn6*Δ*9 tup1*Δ (KKY143)[a]	Komachi et al., 1994
MHY479	*MAT*α *mf**a**2:lacZ trp1 leu2 ura3 his4* (SM1196)[a]	Komachi et al., 1994
MHY481	*mat*αΔ *trp1 leu2 ura3 his4 ura3::URA3::STE6operator-lacZ* (KKYLX7)[a]	Komachi et al., 1994
MHY486	*mat*α*2-aX182 trp1 leu2 ura3 his4* (KT53)[a]	Tatchell et al., 1981
MHY487	*mat**a**1-**a**X20 trp1 leu2 ura3 his4* (KT150)[a]	Tatchell et al., 1981
MHY488	*MAT**a** trp1 leu2 ura3 his4* (EG1-23/KT146)[a]	Tatchell et al., 1981
MHY489	*MAT*α *trp1 leu2 ura3 his4* (246.1.1/KT43)[a]	Tatchell et al., 1981
MHY495	*MAT*α *his3-*Δ*200 leu2-3,112 ura3-52 lys2-801 trp1-1 ubc6::HIS3*	Chen et al., 1993
MHY500	*MAT**a** his3-*Δ*200 leu2-3,112 ura3-52 lys2-801 trp1-1*	Chen et al., 1993
MHY501	*MAT*α *his3-*Δ*200 leu2-3,112 ura3-52 lys2-801 trp1-1*	Chen et al., 1993
MHY503	*MAT*α *his3-*Δ*200 leu2-3,112 ura3-52 lys2-801 trp1-1 ubc4::HIS3 ubc6::HIS3*	Chen et al., 1993
MHY508	*MAT*α *his3-*Δ*200 leu2-3,112 ura3-52 lys2-801 trp1-1 ubc4::HIS3 ubc5::LEU2*	Chen et al., 1993
MHY892	*mat**a**1/MAT*α (MHY487 × MHY489)	This study
MHY940	*MAT**a**/mat*α*2* (MHY488 × MHY486)	This study
MHY949	*MAT**a**/MAT*α (MHY488 × MHY489)	This study
MHY1131	*mat*α*2::LEU2 his3-*Δ*200 leu2-3,112 ura3-52 lys2-801 trp1-1 ubc4-*Δ*1::HIS3 ubc6-*Δ*1::HIS3*	This study
MHY1147	*mat*α*2::LEU2 his3-*Δ*200 leu2-3,112 ura3-52 lys2-801 trp1-1*	This study

[a] Indicates original name(s) for strain.

at the XhoI site. The disruption allele was introduced into MHY503. The resulting strain, MHY1131, was transformed with YCplac33-MATα and crossed to MHY500. MHY1147 was derived from the resulting diploid.

Mutagenesis of the *Deg1* Signal

Deletion analysis of the *Deg1* element was done by oligonucleotide-directed mutagenesis (Ausubel et al., 1989). The mutated *Deg1-lacZ* alleles were transferred into high-copy shuttle vectors; all alleles were verified by DNA sequencing. The plasmid pLR20 used for point mutagenesis of *Deg1* was made as follows. A HindIII/EcoRI fragment carrying *mat*α*X38* (Tatchell et al., 1981) was subcloned into YEplac195. A SalI fragment bearing the *E. coli lacZ* gene from pMC1871 was inserted at the unique XhoI linker site in *mat*α*X38*, yielding pLR1, which encodes an in-frame fusion of the first 67 residues of α2 with βgal. The pLR1 plasmid was used as a template to generate a 0.43 kb HindIII/SmaI PCR fragment that included the upstream α*2* regulatory region (to −219 relative to the start codon, with the introduction of both a HindIII site upstream of this position and an XbaI site at −109) and extended through the SmaI site at the α*2-lacZ* junction in pLR1. The HindIII/SmaI fragment was cloned into YCplac33, yielding pLR19. Finally, a SmaI/ScaI *lacZ* fragment from pLR1 was inserted into the SmaI site of pLR19, yielding pLR20.

For random mutagenesis of α2 residues 1–67, we employed mutagenic PCR amplification of *Deg1*-encoding DNA followed by transformation of yeast cells with the PCR products along with a gapped pLR20 plasmid. The plasmid and PCR fragments can recombine in vivo to regenerate circular plasmids that carry potentially mutant *Deg1-lacZ* alleles (Muhlrad et al., 1992). Mutations that resulted in higher βgal activity were identified by replica-screening on plates containing X-gal. Colonies that express wild-type *Deg1*-βgal are pale blue, whereas degradation mutants are dark blue. From 6 × 10^3 transformants, 41 colonies showed enhanced blue color. Candidates were tested quantitatively for βgal activity using the substrate ONPG. The *Deg1*-encoding regions were sequenced by cycle sequencing of DNA directly isolated from yeast colonies using the *fmol* DNA Sequencing System (Promega). After template amplification, dideoxy sequencing was done with an internal primer that had been 5′-end labeled with [^{32}P]γ-dATP and polynucleotide kinase. Of 41 plasmids sequenced, 36 had mutations (mean: 0.9 mutations/plasmid). Of the 36 mutations, 34 occurred at a T, and 31 of these resulted in a T-to-C transition. Mutations that resulted in high ONPG levels are discussed in the Results. The L23P, C33G, L39S, E48G, and F57S mutations, each isolated only once, resulted in relatively weak elevation of βgal levels (<3×) when measured by quantitative activity assays. The remaining sequenced plasmids carried either no mutation in *Deg1* or silent mutations. Qualitative βgal assays revealed little or no enhancement of enzyme levels in these cases (<2-fold). In subsequent screens, either dGTP, dTTP, or dCTP was lowered to 0.2 mM while the other three deoxynucleotides were added to 1 mM. Similar mutational biases were observed in all the screens, as reported previously (Muhlrad et al., 1992). The latter three screens, totaling ~5 × 10^3 transformants, yielded primarily the same mutations found with dATP limitation.

For cassette mutagenesis of the DNA encoding α2 residues 10–37, a family of 101-base oligonucleotides was synthesized (Keystone Laboratories) such that all had a BglII site at the 5′-end and a HindIII site at the 3′-end, but between these two recognition sites the sequences, which derived from α*2* residues +27 to +111, potentially included one or more base substitutions. The 3′ ends of these oligonucleotides were annealed to one another to prime DNA synthesis by Klenow polymerase. The resulting double-stranded fragments were digested with BglII and HindIII and ligated into the BglII/HindIII-cut, *Deg1*-lacZ bearing pLR23 plasmid; the products were transformed into *E. coli*, creating a library of ~10^3 clones. DNA from this library was isolated, transformed into yeast MHY501, and colonies were screened as described for the random mutagenesis experiments. A level of 1.7% incorrect base incorporation was chosen so that 57% of the fragments were expected to have zero or one substitution (Reidhaar-Olson et al., 1991). For unknown reasons, the number of substitutions actually observed averaged 2.6, resulting in the majority of sequences having multiple amino acid changes (47 of the 54 sequenced).

Pulse-Chase Analysis

Pulse-chase experiments were performed as described (Chen et al., 1993). To detect ubiquitinated $\alpha 2_{101}$, yeast cells were cotransformed with YEp96 or YEp105 plasmids, which express wild-type or myc epitope–tagged Ub, respectively (Ellison and Hochstrasser, 1991). Immunoprecipitations of α2 or $\alpha 2_{101}$ were done with anti-α2 antibodies (Hochstrasser and Varshavsky, 1990), those of **a**1 with an anti-**a**1 antibody (Goutte and Johnson, 1993).

Acknowledgments

We thank A. D. Johnson for strains, plasmids, and anti-**a**1 antibody; E. Reisinger and C. Wolberger for communicating unpublished data; and J. Laney, C. Richardson, R. Rylaarsdam, S. Swaminathan, and A. Turkewitz for critiques of the manuscript. This work was supported by National Institutes of Health (NIH) grant GM46904. P. R. J. was funded by an NIH Underrepresented Minorities grant. P. R. J. and R. S. were supported in part by NIH training grant GM07183.

Received April 24, 1998; revised June 17, 1998.

References

Ausubel, F.M., Brent, R., Kingston, R.E., Moore, D.D., Seidman, J.G., Smith, J.A., and Struhl, K. (1989). Current Protocols in Molecular Biology (New York: John Wiley and Sons).

Bonifacino, J.S., Cosson, P., and Klausner, R.D. (1990). Colocalized transmembrane determinants for ER degradation and subunit assembly explain the intracellular fate of TCR chains. Cell *63*, 503–513.

Campanero, M.R., and Flemington, E.K. (1997). Regulation of E2F through ubiquitin-proteasome-dependent degradation: stabilization by the pRB tumor suppressor protein. Proc. Natl. Acad. Sci. USA *94*, 2221–2226.

Chen, P., Johnson, P., Sommer, T., Jentsch, S., and Hochstrasser, M. (1993). Multiple ubiquitin-conjugating enzymes participate in the in vivo degradation of the yeast MATα2 repressor. Cell *74*, 357–369.

Ellison, M.J., and Hochstrasser, M. (1991). Epitope-tagged ubiquitin: a new probe for analyzing ubiquitin function. J. Biol. Chem. *266*, 21150–21157.

Glotzer, M., Murray, A.W., and Kirschner, M.W. (1991). Cyclin is degraded by the ubiquitin pathway. Nature *349*, 132–138.

Gottesman, S. (1996). Proteases and their targets in Escherichia coli. Annu. Rev. Genet. *30*, 465–506.

Goutte, C., and Johnson, A.D. (1993). Yeast **a**1 and α2 homeodomain proteins form a DNA-binding activity with properties distinct from those of either protein. J. Mol. Biol. *233*, 359–371.

Hall, M.N., and Johnson, A.D. (1987). Homeo domain of the yeast repressor α2 is a sequence-specific DNA-binding domain but is not sufficient for repression. Science *237*, 1007–1012.

Harashima, S., Miller, A.M., Tanaka, K., Kusumoto, K., Tanaka, K., Mukai, Y., Nasmyth, K., and Oshima, Y. (1989). Mating-type control in Saccharomyces cerevisiae: isolation and characterization of mutants defective in repression by **a**1-α2. Mol. Cell. Biol. *9*, 4523–4530.

Herskowitz, I., Rine, J., and Strathern, J. (1992). Mating-type determination and mating-type interconversion in *Saccharomyces cerevisiae*. In The Molecular and Cellular Biology of the Yeast *Saccharomyces*: Gene Expression, E.W. Jones, J.R. Pringle, and J.R. Broach, eds. (Cold Spring Harbor, New York: Cold Spring Harbor Laboratory Press), pp. 583–656.

Ho, Y.-C., Adamson, J.G., Hodges, R.S., and Smith, M. (1994). Heterodimerization of the yeast MAT**a**1 and MATα2 proteins is mediated by two leucine zipper-like coiled-coil motifs. EMBO J. *13*, 1403–1413.

Hochstrasser, M. (1996). Ubiquitin-dependent protein degradation. Annu. Rev. Genet. *30*, 405–439.

Hochstrasser, M., and Varshavsky, A. (1990). In vivo degradation of a transcriptional regulator: the yeast α2 repressor. Cell *61*, 697–708.

Kellerman, K.A., Mattson, D.M., and Duncan, I. (1990). Mutations affecting the stability of the *fushi tarazu* protein of *Drosophila*. Genes Dev. *4*, 1936–1950.

King, R.W., Glotzer, M., and Kirschner, M.W. (1996). Mutagenic analysis of the destruction signal of mitotic cyclins and the structural characterization of ubiquitinated intermediates. Mol. Biol. Cell *7*, 1343–1357.

Komachi, K., Redd, M., and Johnson, A.D. (1994). The WD repeats of Tup1 interact with the homeodomain protein α2. Genes Dev. *8*, 2857–2867.

Kopski, K.M., and Huffaker, T.C. (1997). Suppressors of the *ndc10-2* mutation: a role for the ubiquitin system in Saccharomyces cerevisiae kinetochore function. Genetics *147*, 409–420.

Kornitzer, D., Raboy, B., Kulka, R.G., and Fink, G.R. (1994). Regulated degradation of the transcription factor Gcn4. EMBO J. *13*, 6021–6030.

Li, T., Stark, M.R., Johnson, A.D., and Wolberger, C. (1995). Crystal structure of Mat**a**1/Matα2 homeodomain heterodimer bound to DNA. Science *270*, 262–269.

Lupas, A. (1996). Coiled coils: new structures and new functions. Trends Biochem. Sci. *21*, 375–382.

Magin, T.M., Schröder, R., Leitgeb, S., Wanninger, F., Zatloukal, K., Grund, C., and Melton, D.W. (1998). Lessons from keratin 18 knockout mice: formation of novel keratin filaments, secondary loss of keratin 7 and accumulation of liver-specific keratin 8-positive aggregates. J. Cell Biol. *140*, 1441–1451.

Mann, R.S., and Chan, S.K. (1996). Extra specificity from extradenticle: the partnership between HOX and PBX/EXD homeodomain proteins. Trends Genet. *12*, 258–262.

Muhlrad, D., Hunter, R., and Parker, R. (1992). A rapid method for localized mutagenesis of yeast genes. Yeast *8*, 79–82.

Rechsteiner, M., and Rogers, S.W. (1996). PEST sequences and regulation by proteolysis. Trends Biochem. Sci. *21*, 267–271.

Reidhaar-Olson, J.F., Bowie, J.U., Breyer, R.M., Hu, J.C., Knight, K.L., Lim, W.A., Mossing, M.C., Parsell, D.A., Shoemaker, K.R., and Sauer, R.T. (1991). Random mutagenesis of protein sequences using oligonucleotide cassettes. Meth. Enzymol. *208*, 564–586.

Sadis, S., Atienza, C., and Finley, D. (1995). Synthetic signals for ubiquitin-dependent proteolysis. Mol. Cell. Biol. *15*, 1265–1273.

Sauer, R.T., Smith, D.L., and Johnson, A.D. (1988). Flexibility of the yeast α2 repressor enables it to occupy the ends of its operator, leaving the center free. Genes Dev. *2*, 807–816.

Sommer, T., and Wolf, D.H. (1997). Endoplasmic reticulum degradation: reverse protein flow of no return. FASEB J. *11*, 1227–1233.

Tatchell, K., Nasmyth, K.A., Hall, B.D., Astell, C., and Smith, M. (1981). In vitro mutation analysis of the mating-type locus in yeast. Cell *27*, 25–35.

Treier, M., Staszewski, L.M., and Bohmann, D. (1994). Ubiquitin-dependent c-jun degradation in vivo is mediated by the δ domain. Cell *78*, 787–798.

Varshavsky, A. (1997). The ubiquitin system. Trends Biochem. Sci. *22*, 383–387.

Vershon, A.K., Jin, Y., and Johnson, A.D. (1995). A homeo domain protein lacking specific side chains of helix 3 can still bind DNA and direct transcriptional repression. Genes Dev. *9*, 182–192.

Wang, W., Chevray, P.M., and Nathans, D. (1996). Mammalian Sug1 and c-Fos in the nuclear 26S proteasome. Proc. Natl. Acad. Sci. USA *93*, 8236–8240.

Yaron, A., Gonen, H., Alkalay, I., Hatzubai, A., Jung, S., Beyth, S., Mercurio, F., Manning, A.M., Ciechanover, A., and Ben-Neriah, Y. (1997). Inhibition of NF-κB cellular function via specific targeting of the IκB-ubiquitin ligase. EMBO J. *16*, 6486–6494.